Defects in synthesized and natural diamond probed by positron annihilation

1999 J. Phys.: Condens. Matter 11 4109

(http://iopscience.iop.org/0953-8984/11/20/317)

J. Phys.: Condens. Matter **11** (1999) 4109–4122. Printed in the UK PII: S0953-8984(99)97818-9

Defects in synthesized and natural diamond probed by positron annihilation

A Uedono†, S Fujii‡, N Morishita§, H Itoh§, S Tanigawa† and S Shikata‡

† Institute of Materials Science, University of Tsukuba, Tsukuba, Ibaraki 305-8573, Japan
‡ Itami Research Laboratories, Sumitomo Electric Industries Limited, 1-1-1 Koya-kita, Itami 664-0016, Japan
§ Japan Atomic Energy Research Institute, 1233 Watanuki, Takasaki, Gunma 370-1292, Japan

Received 25 September 1998, in final form 12 November 1998

Abstract. Defects in synthesized and natural diamond were studied using the positron annihilation technique. For a synthesized type IIa specimen, the lifetime of positrons annihilating from the free state was determined to be 98.7 ps. For a synthesized type Ib specimen, the effects of the annihilation of positrons trapped by open spaces introduced by substitutional nitrogen atoms on the positron parameters were discussed. After electron irradiation, the species of the major vacancy-type defects was identified to be a neutral and/or negatively charged monovacancy. For natural type IIa and IIb specimens, the annihilation mode of positrons trapped by vacancy clusters was observed. For the natural type IIb specimen, the temperature dependence of the trapping rate of the vacancy clusters was explained assuming that these clusters act as compensators for acceptor impurities (boron).

1. Introduction

A great number of studies on the nature of diamond have been carried out because of its excellent optical and electrical properties [1]. Since diamond is transparent from the infra-red to the ultra-violet regions, except for absorption bands due to lattice vibrations, it has a high potential for use in optical components. For high-heat-load optical components such as are used in synchrotron radiation systems, diamond single crystals were reported to be superior to other monochromator materials [2]. Diamond has also been attracting interest as a potential material for high-frequency and high-power application in high-temperature operation [3]. Since the diffusion coefficients of all known dopants are extremely low in diamond, the most promising doping technique is ion implantation [4]. However, the fabrication of diamond devices using ion implantation is not easy. One of the main difficulties is the high annealing temperatures of defects introduced by ion implantation. To find annealing processes that can be used without causing graphitization, knowledge of the properties of the defects is crucial. Since radiation damage introduces colour centres [1], the study of defects is also important for the fabrication of optical devices using diamond. In the present paper, we used the positron annihilation technique to study native defects and electron-irradiation-induced defects in synthesized and natural diamond.

The positron annihilation technique is regarded as a powerful means of studying defects in metals and semiconductors [5]. Using this technique, native defects and irradiation-induced defects in diamond have been studied [6–10]. However, for diamond, the behaviour of positrons trapped by vacancy aggregates or impurity-related defects is not established as is

0953-8984/99/204109+14$19.50

the case for other semiconductors. In the present work, the annihilation characteristics of positrons in various diamond specimens were systematically studied. From another point of view, the annihilation characteristic of positrons from the free state attracts attention, because, for diamond, the electron–positron momentum distribution observed by means of angular correlation of annihilation radiation (ACAR) is very different from that for other semiconductors such as Si and Ge [11, 12]. Contrary to those for diamond, ACAR spectra for Si and Ge show a deep dip around the Γ point. Using first-principles calculations or density-functional theory [13–16], the observed difference between the ACAR spectra for diamond and other group-IV semiconductors was successfully explained in terms of the small diamond lattice constant and the weak electron–positron correlation effects in diamond. In the present work, it was found that nitrogen atoms act as trapping centres for positrons, and affect the momentum distribution of positron–electron pairs. Since nitrogen atoms are the major impurities in diamond, the study of the interaction between positrons and nitrogen atoms can provide useful information on the electron–positron momentum density distribution in diamond.

2. Experimental procedure

The synthesized single crystals of diamond (type Ib and IIa) used in the present experiments were grown at Sumitomo Electric Industries; a qualitative classification system for diamond was explained in reference [1]. By the double-crystal x-ray diffraction method, the crystallographic quality of the specimens was found to be close to the level for commercial Si single crystals [17]. The concentration of nitrogen atoms in the type Ib specimens was estimated to be 10–120 ppm. The synthesized specimens were irradiated with 3 MeV electrons up to a dose of 1×10^{18} cm^{-2}. During the irradiation, the temperature of the specimens was kept below 360 K. Natural diamond specimens (type Ia, IIa and IIb) were also studied. In the present experiments, all specimens were cut from crystals along ⟨100⟩ directions.

The basic concept of the positron annihilation technique is explained as follows. In condensed matter, a positron annihilates with an electron mainly into two γ-quanta. The annihilation line is broadened due to the momentum component of the annihilating electron–positron pair, P_L, parallel to the direction of the emitted annihilation γ-quantum. The energy of the γ-rays is given by the relation $E_\gamma = 511 \pm \Delta E$ keV. The Doppler shift, ΔE, is obtained from the relation $\Delta E = P_L c/2$, where c is the speed of light. When a positron is trapped by vacancy-type defects, the annihilation probability of positrons with core electrons decreases and hence that of positrons with valence electrons increases. Because the momentum distribution of core electrons is broader than that for valence electrons, the Doppler broadening spectrum is narrowed by the trapping of positrons by vacancy-type defects. The energy distribution of γ-rays corresponding to the annihilation of positrons with valence electrons is also affected by the trapping of positrons by defects [12]. The change in the Doppler broadening spectrum is characterized by the S-parameter, which is the ratio of counts in the central region of the spectrum to the total counts [18]. When positrons are trapped by vacancy-type defects, both the decrease in the fraction of positrons annihilating with core electrons and the change in the momentum distribution corresponding to the annihilation of positrons with valence electrons increase the value of S.

The lifetime of positrons, τ, is expressed by

$$1/\tau \propto \int \rho_+(\rho_v + \rho_c)\, dr$$

where ρ_+, ρ_v and ρ_c are the total charge densities of positrons, valence and core electrons,

respectively. When a positron is trapped by vacancy-type defects, the decrease of ρ_c in such a region increases τ. Since the relationship between lifetimes and the species of defects has been established [19], one can identify defects from measurements of lifetime spectra of positrons and calculations.

In the present experiments, Doppler broadening spectra of the annihilation radiation and lifetime spectra of positrons were measured with increasing specimen temperature from 20 K to 290 K in the dark. In these measurements, high-energy positrons ($\leqslant$0.54 MeV) emitted from ^{22}Na were directly implanted into the specimens. Doppler broadening spectra were measured by a Ge detector, and they were characterized by the *S*-parameter; the central region of the spectrum was defined as 511 ± 0.8 keV. Lifetime spectra were measured by a fast–fast system with BaF_2 scintillators attached to XP2020Q photomultiplier tubes. The full width at half-maximum (FWHM) of the time resolution was about 200 ps. At each temperature, the Doppler broadening spectrum and the lifetime spectrum contained about 1×10^7 counts and about 1×10^6 counts, respectively. The lifetime spectrum of positrons, $I(t)$, is expressed by

$$I(t) = \sum \lambda_i I_i \exp(-\lambda_i t) \tag{1}$$

where λ_i and I_i are the annihilation rate of positrons of the ith component and its intensity, respectively. The ith lifetime component, τ_i, is given by $1/\lambda_i$. In the present experiments, the observed lifetime spectra were analysed using the computer program RESOLUTION [20].

The implantation profile of monoenergetic positrons can be adjusted to a restricted region of interest in the specimen by accelerating them to the desired energy [21]. In the present work, a monoenergetic positron beam is used to measure the diffusion length of positrons in the specimens. Doppler broadening spectra were measured with a Ge detector as a function of incident positron energy, E, at room temperature. A spectrum with a total count of 5×10^5 was measured for each incident positron energy. The observed relationship between the *S*-parameter and E was analysed using a computer code, VEPFIT, developed by van Veen *et al* [22]. The one-dimensional diffusion model of positrons is expressed as

$$D_+ \frac{d^2}{dz^2} n(z) - \kappa_{\text{eff}} n(z) + P(z, E) = 0 \tag{2}$$

where D_+ is the diffusion coefficient of positrons, $n(z)$ is the probability density of positrons at a distance z from the surface, κ_{eff} is the effective rate of escape of positrons from the diffusion process and $P(z, E)$ is the implantation profile of positrons [21]. κ_{eff} is related to the concentration of defects C_d by $\kappa_{\text{eff}} = \lambda_f + \mu_d C_d$, where λ_f is the rate of annihilation of positrons from the free state and μ_d is the specific positron trapping rate of the defect. The diffusion length of positrons, L_d, is given by

$$L_d = \sqrt{D_+/\kappa_{\text{eff}}}. \tag{3}$$

VEPFIT solves equation (2) and gives the fractions of positrons annihilated at the surface, $F_s(E)$. The observed *S*–*E* curves were fitted to

$$S(E) = S_s F_s(E) + S_b[1 - F_s(E)] \tag{4}$$

where S_s and S_b are the characteristic values of the *S*-parameter for positrons annihilating at the surface and in the bulk, respectively.

3. Results and discussion

3.1. Annihilation characteristics of positrons in the synthesized diamond (Ib and IIa) before electron irradiation

Figures 1 and 2 show the temperature dependence of the *S*-parameter and that of the lifetime of positrons for the synthesized type Ib and IIa specimens, respectively; the lifetime spectra were

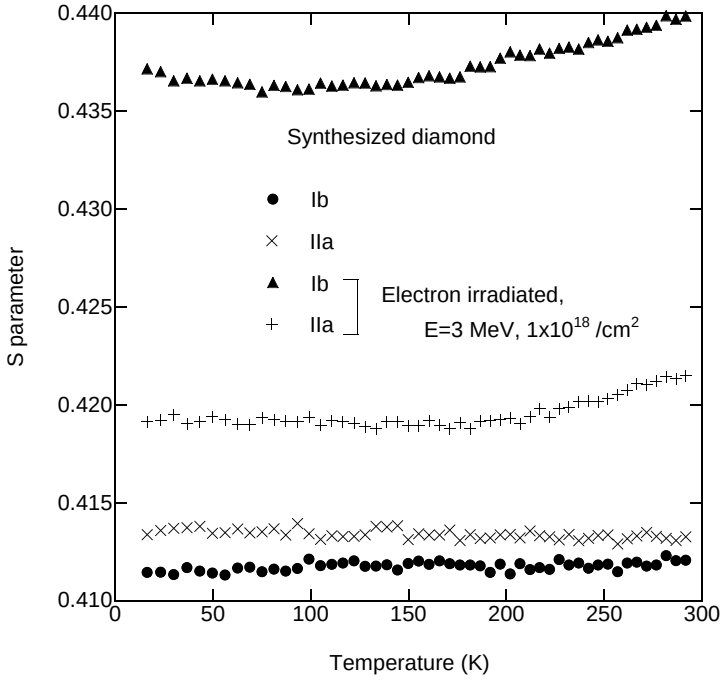

Figure 1. The *S*-parameter for the synthesized type Ib and IIa specimens before and after electron irradiation as a function of temperature. The increase of *S* observed for the electron-irradiated specimens is attributed to the annihilation of positrons trapped by monovacancies introduced by the irradiation.

analysed assuming one annihilation mode, so the mean lifetime of positrons was given. In figures 1 and 2, for both specimens, *S* and the lifetime of positrons are almost constant over the temperature range for which measurements were made. The average lifetimes were calculated to be 106 ps and 98.7 ps for the type Ib and IIa specimens, respectively. From measurements of lifetime spectra of positrons for type Ia diamond, Dannefaer *et al* [6] reported that the lifetime of positrons annihilating from the free state, τ_f, is about 120 ps. In their experiments, since the annihilation mode caused by the trapping of positrons by vacancy-type defects was observed, τ_f was obtained using the two-state trapping model for positrons. The value of τ_f estimated using this model could include some uncertainty, but is close to the theoretical value of 114 ps reported by Puska *et al* [19]. Li *et al* [23] successfully analysed the lifetime spectrum for type IIa diamond by assuming one annihilation mode, and τ_f was determined to be 97.5 ps. Recently, from theoretical calculations using *ab initio* pseudopotentials [15], τ_f was determined to be 93–96 ps. These values are close to the lifetime of positrons obtained for the type IIa specimen in the present experiments.

For the type Ib specimen, the lifetime of positrons obtained is longer than that for the type IIa specimen. Assuming that τ_f is close to the lifetime of positrons for the type IIa specimen, the observed increase of the lifetime for the type Ib specimen might be attributed to the trapping of positrons by vacancy-type defects. In figure 1, *S* for the type Ib specimen is smaller than that for the type IIa specimen. As discussed in section 2, the trapping of positrons by vacancy-type defects increases both the lifetime of positrons and *S*. Thus, the observed increase of the lifetime of positrons for the type Ib specimen cannot be attributed to the annihilation of positrons by 'pure' vacancy-type defects.

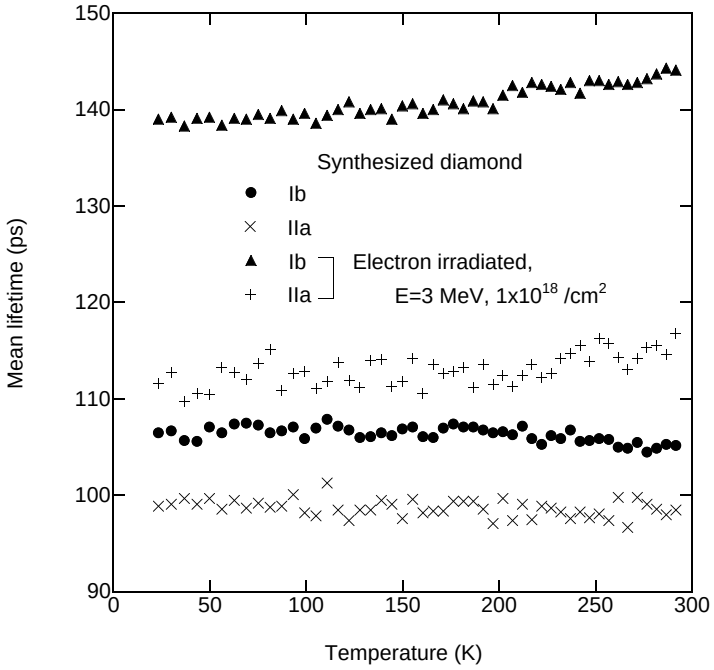

Figure 2. The lifetime of positrons for the synthesized type Ib and IIa specimens before and after electron irradiation as a function of temperature. The lifetime spectra of positrons for the type IIa specimen after electron irradiation were decomposed into two components, and the calculated mean lifetime of positrons is shown in the figure. The lifetime spectra for the other specimens were analysed assuming one annihilation mode.

In order to know the behaviour of positrons in more detail, the relationship between the S-parameter and E for the synthesized specimens was measured. Figure 3 shows the S-parameter as a function of E for the type Ib and IIa specimens [8]. In figure 3, S was found to approach a constant value at high E ($<$20 keV). This indicates that almost all positrons are implanted into the bulk in this energy range and annihilated in the bulk without diffusing back to the surface of the specimen. For each specimen, the value of S at $E > 20$ keV is different from that of S measured using high-energy positrons (figure 1). This is mainly due to the difference in the experimental conditions in the different measurements. In this energy region, S for the type Ib specimen is smaller than that for the type IIa specimen. This relationship agrees with that shown in figure 1. The observed increase of S at low E ($\simeq$0 keV) is attributed to the annihilation of positrons and that of positronium at the surface of the specimen; the characteristic values of S for these annihilation modes are larger than S corresponding to the annihilation of positrons in the bulk [21]. The observed S–E curves were fitted by equation (4). In figure 3, the solid curves are the result of the fitting. From the fitting, the values of L_{d} were determined to be 52.1 ± 0.4 nm and 100 ± 1 nm for the type Ib and IIa specimens, respectively. L_{d} for the type IIa specimen is close to that for Si with no defect response (130–250 nm) [21, 24]. Thus, the short diffusion length of positrons obtained for the type Ib specimen can be attributed to the trapping or the scattering of positrons by defects; the agreement between the data and the fitting curve suggests that the distribution of such centres is homogeneous in the region probed by monoenergetic positrons. Therefore, it can be concluded that τ_{f} is close to (or lower than) the lifetime of positrons for the type IIa specimen (98.7 ps).

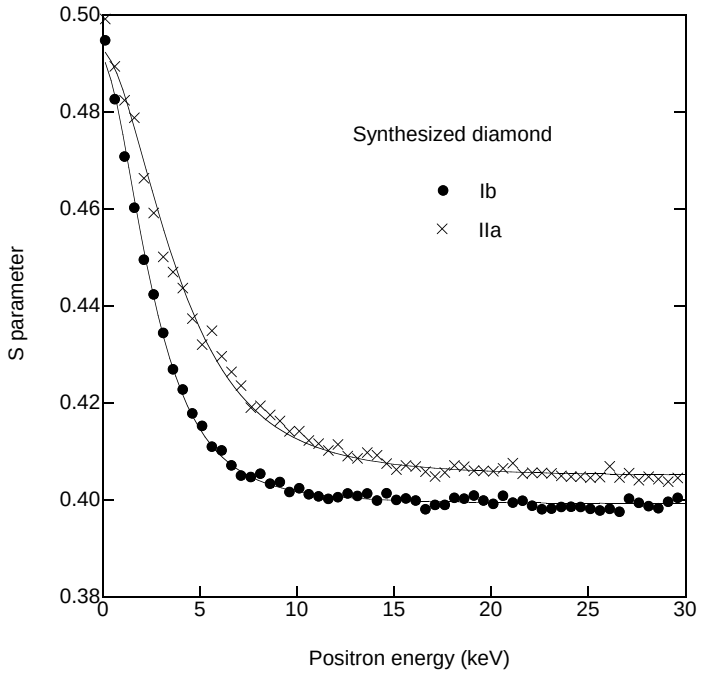

Figure 3. The S-parameter as a function of incident positron energy for the synthesized type Ib and IIa specimens. The solid curves are fits of equation (4) to the experimental data. From the fitting, the values of L_d were determined to be 52.1 ± 0.4 nm and 100 ± 1 nm for the type Ib and IIa specimens, respectively.

According to the trapping model of positrons [18], the fraction of positrons trapped by defects, F_d, can be calculated as $F_d = \mu_d C_d/(\lambda_f + \mu_d C_d)$. Using equation (3), the relation between F_d and L_d is obtained to be $F_d = 1 - (L_{d(defect)}/L_{d(free)})^2$, where $L_{d(free)}$ is the diffusion length of positrons in the defect-free specimen. Assuming $L_{d(free)}$ is close to L_d determined for the type IIa specimen, F_d for the type Ib specimen was calculated to be 0.7. According to Puska *et al* [19], the lifetime of positrons trapped by monovacancies, V, was calculated to be 146 ps. The observed lifetime of positrons for the type Ib specimen (106 ps) cannot be represented assuming that the trapping centres of positrons in the type Ib specimen are vacancy-type defects. This conclusion was obtained assuming that the concentration of defects in the region probed by monoenergetic positrons is same as that in the region probed by high-energy positrons.

The major impurity of type Ib diamond is known to be nitrogen. The nature of dispersed substitutional nitrogen atoms in diamond has been studied from measurements of electron spin resonance (ESR) [25]. In the present experiments, in order to confirm the configuration of nitrogen atoms in the type Ib specimen, ESR spectra were measured at room temperature using an X-band (9 GHz) microwave incident on a TE_{011} cylindrical cavity. Figure 4 shows typical ESR spectra for the type Ib specimen; the magnetic field was applied along $\langle 100 \rangle$ axis. Isoya [26] reported ESR spectra for synthesized type Ib diamond provided by Sumitomo Electric Industries. In his report, the observed spectra were almost identical to those obtained in the present experiments. Thus, identification of the lines shown in figure 4 was performed according to his report. In figure 4(a), the three major lines are associated with the hyperfine (hf) interaction of ^{14}N (nuclear spin, $I = 1$; natural abundance $= 99.63\%$). Figure 4(b) shows

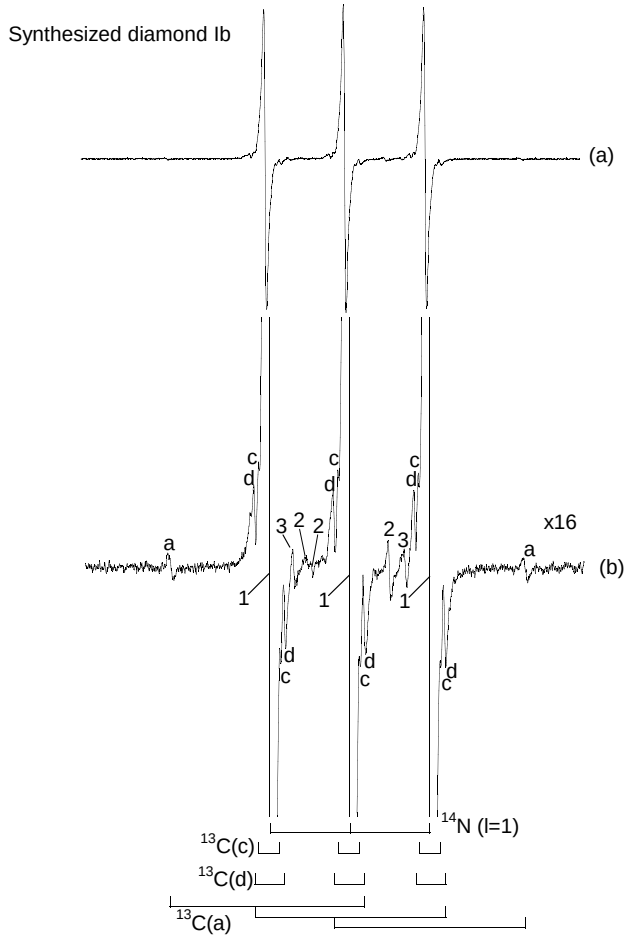

Figure 4. The ESR spectra for the synthesized type Ib specimen; the magnetic field was applied parallel to the ⟨100⟩ axis. (a) The three major lines are associated with the hf interaction of ^{14}N ($I = 1$, 99.63%). (b) The hf interaction between the paramagnetic electron and ^{13}C ($I = 1/2$, 1.11%) nuclei. Labels 1, 2 and 3 correspond to the hf lines with ^{14}N, those related to the forbidden transition due to the ^{14}N quadrupole moment and those with ^{15}N ($I = 1/2$, 0.37%), respectively.

the hf interaction between the paramagnetic electron and ^{13}C ($I = 1/2$, 1.11%) nuclei; the labels of ^{13}C (a, c and d) correspond to the positions of carbon atoms shown in figure 1 in the review paper written by Loubser and van Wyk [25]. Labels 1, 2 and 3 correspond to the hf lines with ^{14}N, those related to the forbidden transition due to the ^{14}N quadrupole moment and those with ^{15}N ($I = 1/2$, 0.37%), respectively. The spectra were also measured as a function of the direction of the magnetic field, and the observed anisotropy agreed with that reported by Smith *et al* [27]. These results suggest that the paramagnetic electron is localized on the C–N bond, and this electron is accommodated in a C(sp^3)–N(sp^3) antibonding hybrid orbital [25–27]. It was suggested that the C–N bond on which the unpaired electron is situated is about 10–14% longer than the usual C–N bond length; this distortion is interpreted as a manifestation of the Jahn–Teller effect [25].

Because of the lattice distortion near substitutional nitrogen atoms, the positrons could be trapped by such a region and, as a result, the lifetime of positrons could increase. Since the

trapping potential of such a region is expected to be low, the interaction between positrons and the open space introduced by impurities is not fully established at this stage. Krause-Rehberg *et al* [28] observed an increase of the lifetime of positrons due to trapping by DX centres in Te-doped $Al_xGa_{1-x}Sb$; the ground state of DX centres is considered to exhibit the Jahn–Teller distortion. These experimental results suggest the trapping of positrons by the lattice distortion introduced by impurities. From above discussion, the value of S obtained for the type IIa specimen is considered to be close to the characteristic value of S for the annihilation of positrons from the free state, S_f. The observed decrease of S for the type Ib specimen can be attributed to the annihilation of positrons near substitutional nitrogen atoms. From several experiments performed by Uedono and co-workers [29, 30], it was established that the characteristic value of S for vacancy–oxygen complexes is smaller than S_f. They suggested that S is decreased by the annihilation of positrons with electrons of oxygen atoms. For the present experiments, therefore, the observed decrease of S is attributable to the annihilation of positrons with electrons of nitrogen atoms.

One can estimate the charge state of defects from the temperature dependence of the trapping rate for these defects. The model which describes the trapping of positrons by charged vacancies in semiconductors was developed by Puska *et al* [31]. In this model, a positron is trapped into a Rydberg state by the emission of a phonon, and the transition into the ground state occurs via electron–hole excitation processes. According to this model, μ_d for neutral vacancies is almost independent of temperature. For negatively charged vacancies, μ_d is larger than that for neutral ones, and the difference is enhanced at low temperature. As shown in figures 1 and 2, the values of S and the lifetime of positrons for the type Ib specimen are almost constant. This suggests that the charge state of the trapping centres is neutral. This conclusion agrees with the charge state of substitutional nitrogen atoms in diamond.

3.2. Electron-irradiation-induced defects in the synthesized diamond (Ib and IIa)

The temperature dependencies of S for the electron-irradiated specimens (synthesized Ib and IIa) are shown in figure 1. For the electron-irradiated type Ib specimen, the lifetime spectra of positrons were analysed assuming one annihilation mode. For the electron-irradiated type IIa specimen, the spectra were decomposed into two components, and the mean lifetime of positrons, τ_M, was calculated from the relation $\tau_M = \sum \tau_i I_i$ (see figure 2). For the electron-irradiated specimens, the values of S and the lifetime of positrons are larger than those for the unirradiated ones. This is attributed to the annihilation of positrons trapped by vacancy-type defects introduced by the irradiation.

In figure 2, for the type Ib specimen, the lifetime of positrons obtained is 139–144 ps over the temperature range for which measurements were made. Since the derived lifetime of positrons is close to the lifetime of positrons trapped by V (146 ps), almost all positrons are considered to annihilate from this state. After electron irradiation, for the type IIa specimen, the values of S and the lifetime of positrons are smaller than those for the type Ib specimen. This means that F_d $(=\mu_d C_d/(\lambda_f + \mu_d C_d))$ for the type IIa specimen is lower than that for the type Ib specimen. Since the mechanism of introduction of V in the type IIa specimen is the same as that for the Ib specimen, the concentration of V for the type IIa specimen is considered to be the same as that for the type Ib specimen. For the electron-irradiated type Ib diamond, the complexes formed between V and a nitrogen atom, NV, are known to be formed after about 900 °C annealing [25]. Thus, the effect of NV on S or the lifetime of positrons is considered to be negligible in the present experimental conditions. Therefore, the difference between the results for the type Ib and IIa specimens can be associated with that in μ_d; μ_d depends on the charge state of the defects (see section 3.1).

The irradiation-induced defects in diamond have been studied by optical measurements [1, 32–34]. The optical absorption band, GR1, which consists of a prominent zero-phonon line at 1.673 eV and the phonon-assisted structure at higher energies centred at about 2.0 eV, has been associated with the neutral monovacancy, V^0 [34]. Another prominent band, ND1, which consists of a sharp zero-phonon line at 3.129 eV and the phonon-assisted structure at higher energies centred at about 3.4 eV, is also produced by the irradiation. This band has been variously interpreted as arising from interstitial nitrogen or from negatively charged monovacancies, V^-, but the latter identification seems to be confirmed [34, 35]. While the GR1 centre is a dominant signal for relatively pure diamond (type IIa), an intense signal of the ND1 centre is observed when a sufficient concentration of nitrogen is present in the specimen (type Ia and Ib). The role of nitrogen atoms is to convert the vacancies produced by irradiation from V^0 to V^- by charge transfer from nitrogen 'donors' [25]. Thus, in the present experiments, for the type Ib specimen, the high trapping rate of positrons by vacancy-type defects can be attributed to the attractive long-range Coulomb potential of V^- and the resultant increase of μ_d.

For the type IIa specimen, the derived first and the second lifetimes of positrons, τ_1 and τ_2, and the second intensity, I_2, are shown in figure 5 ($I_1 = 1 - I_2$). On the basis of the trapping model [18], the lifetime of positrons annihilated from the free state, $\tau_{f(cal)}$ was calculated from the relation $1/\tau_{f(cal)} = \sum I_i/\tau_i$. In figure 5, $\tau_{f(cal)}$ was almost constant over the temperature range for which measurements were made; the average value was calculated to be 108 ps. The derived value of $\tau_{f(cal)}$ is longer than the lifetime of positrons obtained for the type IIa specimen (98.7 ps), but, considering the uncertainty in the calculation of $\tau_{f(cal)}$, the difference between τ_f and $\tau_{f(cal)}$ can be judged acceptable. For example, the uncertainty of $\tau_{f(cal)}$ could be caused by an incorporation of two or more annihilation modes into the first annihilation mode.

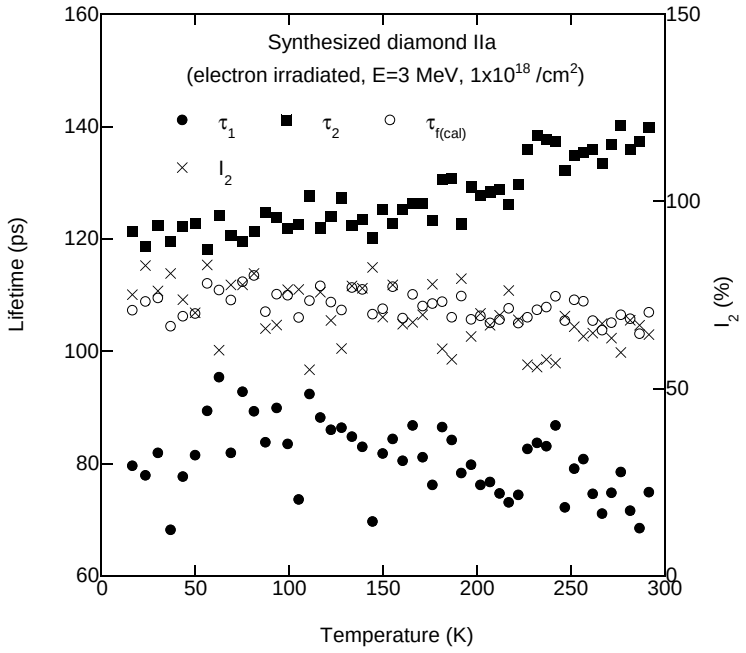

Figure 5. The temperature dependencies of the first and the second lifetimes of positrons, τ_1 and τ_2, and the second intensity, I_2, for the electron-irradiated type IIa specimen (synthesized) as a function of temperature. The calculated lifetime of positrons annihilating from the free state, $\tau_{f(cal)}$ is also shown.

In figure 5, at room temperature, τ_2 is close to the lifetime of positrons trapped by V, but it decreases with decreasing temperature. The difference between the values of τ_2 below 50 K and at room temperature is about 20 ps. The observed increase of τ_2 is almost half of the increase of the lifetime of positrons due to the trapping of positrons by V. Thus, the temperature dependence of τ_2 is unlikely to be associated with the increase in the size of V by thermal expansion. The coexisting defects with the shallow trapping potential could be effective trapping centres for positrons at low temperature. The presence of such shallow trapping centres in electron-irradiated diamond has already been suggested by Dannefaer *et al* [6], but their origin is unknown at this stage. For vacancy-type defects, the trapping potential of positrons decreases with decreasing size of the open volume of such defects. Thus, the observed temperature dependence of τ_2 for the type IIa specimen is likely to be attributable to the trapping of positrons by open spaces, and the size of such spaces is considered to be smaller than that of V. The introduction of small and inhomogeneous amorphous regions or the lattice distortion introduced by the formation of $C(sp^2)$–$C(sp^2)$ hybrid orbitals could be the origin of the shallow traps. In figure 2, for the type Ib specimen, the lifetime of positrons varies from 140 ps to 144 ps in the temperature range between 20 K and 290 K. The observed increase of the lifetime of positrons is smaller than that of τ_2 for the type IIa specimen. The difference between the results for the type Ib and IIa specimens can be attributed to the trapping of positrons by V^- in the type Ib specimen, and a resultant suppression of the trapping of positrons by the shallow traps.

3.3. Vacancy-type defects in natural diamond (Ia, IIa and IIb)

Figure 6 shows the temperature dependence of *S* for the natural type Ia, IIa and IIb specimens. For comparison, the results for the synthesized specimens are also shown in the same figure. For the type Ia specimen, the observed lifetime spectra were analysed assuming one annihilation mode. For the type IIa and IIb specimens, they were decomposed into two components.

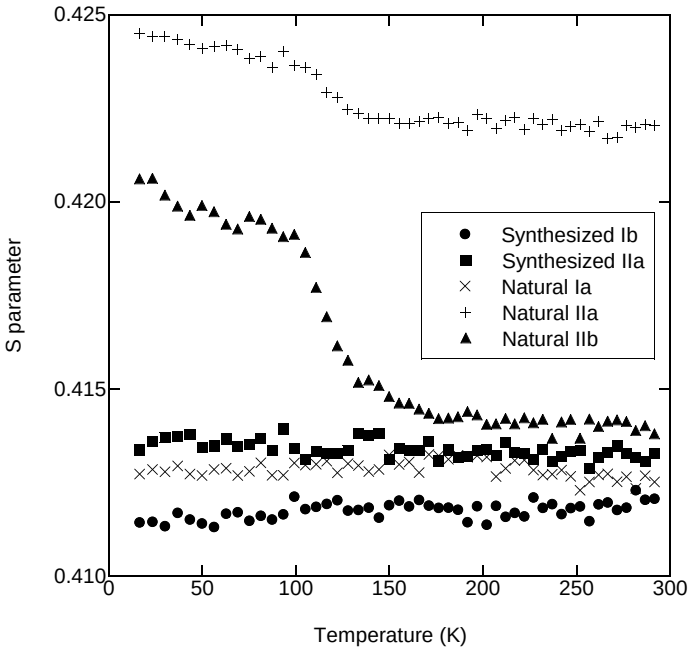

Figure 6. The *S*-parameter for the natural type Ia, IIa and IIb specimens as a function of temperature. The results for the synthesized specimens are also shown.

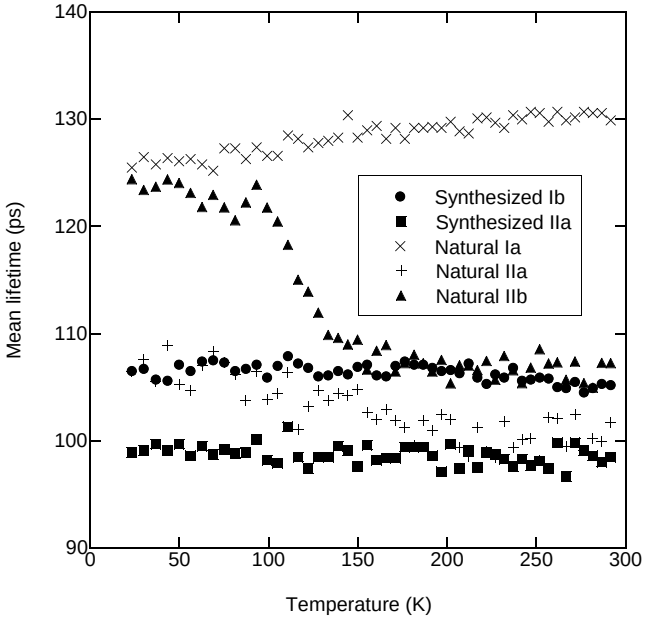

Figure 7. The lifetime of positrons for the natural type Ia, IIa and IIb specimens and the synthesized specimens as a function of temperature. For the natural type Ia specimens, the lifetime spectra were analysed assuming one annihilation mode. For the natural type IIa and IIb specimens, the spectra were decomposed into two components, and the calculated mean lifetime of positrons is shown in the figure.

Figure 7 shows the lifetime results for the type Ia, IIa and IIb specimens. Since the properties of each natural diamond are very individual [1], the discussion in this section is mainly performed qualitatively.

For the type Ia specimen, the lifetime of positrons is longer than that for all of the other specimens, but the value of S is lower than that for the type IIa and IIb specimens. Type Ia diamond is characterized by the presence of appreciable amounts of nitrogen atoms with many forms from isolated substitutionals via simple aggregates to platelets [1]. According to the discussion in section 3.1, the observed long lifetime of positrons can be attributed to the annihilation of positrons trapped by open spaces introduced by substitutional nitrogen atoms, nitrogen aggregates, etc. The small value of S can be attributed to the annihilation of positrons with electrons of nitrogen atoms.

For the type IIa specimen, the derived values of τ_1, τ_2 and I_2 are shown in figure 8. In figure 8, the value of τ_1 is longer than τ_f. This suggests that the annihilation mode corresponding to the trapping of positrons by vacancy-type defects is incorporated into the first component. The value of τ_1 decreased slightly with increasing temperature; the average values of τ_1 below 50 K and above 250 K are 115 ps and 112 ps, respectively. This temperature dependence is considered to correspond to that of S or τ_M (figures 6 and 7). However, since the observed changes of these parameters are small, the defects detected by the second annihilation mode are mainly discussed in the present paper.

In figure 8, τ_2 is almost constant over the temperature range of the measurements, and the average value of τ_2 was calculated to be 397 ps. The relationship between the size of vacancy clusters such as V_3 or V_4 and the lifetime of positrons trapped by such defects is not confirmed at this stage. Since a linear relationship between the lifetime and the size of vacancy-type

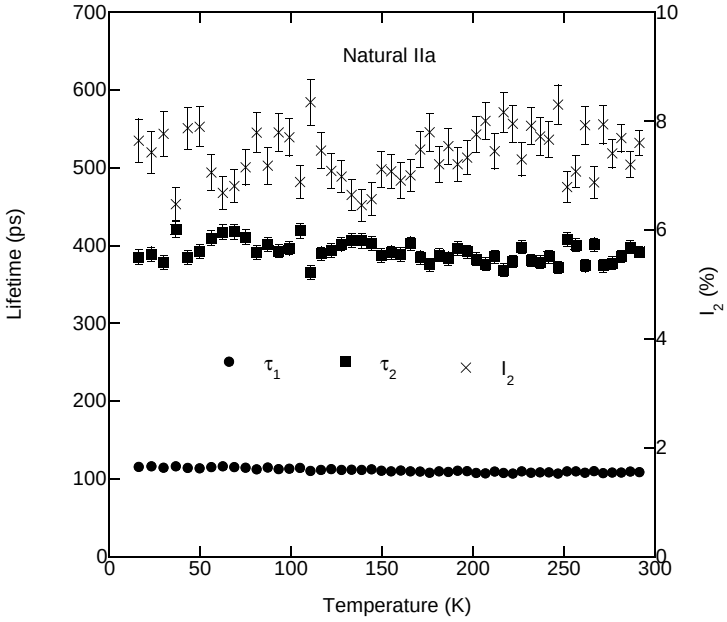

Figure 8. The temperature dependencies of τ_1, τ_2 and I_2 for the natural type IIa specimen as a function of temperature.

defects is known to be obtained for Si and SiC [36, 37], the lifetime of positrons trapped by vacancy clusters in diamond might be extrapolated from a similar relationship. According to this assumption, the size of vacancy-type defects detected by the second component was estimated to be $V_5 - V_6$. The observed temperature dependence of I_2 suggests that the charge state of the vacancy cluster is neutral.

For the type IIb specimen, the derived values of τ_1, τ_2 and I_2 are shown in figure 9. In figure 9, the value of τ_1 and its temperature dependence are close to those for the type IIa specimen. In the temperature range between 125 K and 290 K, the error of τ_2 is large. This is due to the small value of I_2 for this temperature range. Using the value of τ_2 in the temperature range between 20 K and 100 K, the average value of τ_2 was calculated to be 426 ps, and the size of vacancy-type defects detected by the second component was estimated to be $V_6 - V_7$. I_2 is almost constant over the temperature range between 20 K and 100 K, and it starts to decrease above 100 K. Above 150 K, I_2 becomes constant again. As discussed in section 3.1, μ_d for negatively charged defects increases with decreasing temperature, but the observed very sharp increase of I_2 at 100–150 K cannot be represented by the temperature dependence of μ_d for negatively charged defects [31, 38]. Thus, the temperature dependence of I_2 is considered to be due to the change in the charge state of the vacancy clusters. The shift of the charge state from neutral to negative (or positive to neutral) increases the value of μ_d. Thus, the temperature dependence of I_2 might be explained by assuming that these defects act as donors. Since the size of the open space of vacancy clusters observed for the type IIb specimen is close to that for the type IIa specimen, the natures of these defects could be close to each other. Thus, the observed difference in the temperature dependence of I_2 is likely to be attributable to the presence of boron atoms in the type IIb specimen. Assuming that the vacancy clusters act as compensators, such defects could accept holes emitted by the activation of boron atoms. At this stage, because of the difficulty of the determination of the Fermi level for natural diamond, the model fitting of the temperature dependence of I_2 is difficult. But the most probable candidate of the origin for the I_2–T relationship observed for the type IIb specimen is the compensation of carriers by the vacancy clusters. Boron is the

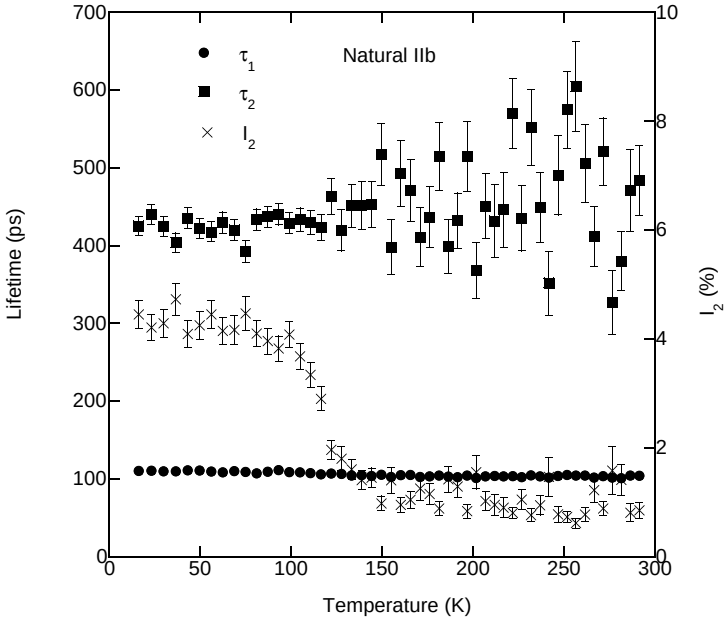

Figure 9. The temperature dependencies of τ_1, τ_2 and I_2 for the natural type IIb specimen as a function of temperature.

major impurity, which can be easily introduced during the growth processes of diamond or diamond-like carbon films fabricated by the chemical vapour deposition technique [1]. The positron annihilation technique has been applied to characterize these thin films [39–42], and those investigations suggested the presence of vacancy clusters with high concentration in the films. Thus, the monitoring of vacancy clusters is important for the fabrication of boron-doped diamond films.

4. Conclusions

We have presented a study of vacancy-type defects in synthesized and natural diamond specimens. The Doppler broadening spectra of the annihilation radiation and the lifetime spectra of positrons were measured over the temperature range between 20 K and 290 K. In order to establish the diffusion length of positrons in the synthesized specimens, Doppler broadening spectra were measured as a function of incident positron energy. For the synthesized type IIa specimen, the observed lifetime of positrons is almost constant over the temperature range for which measurements were made, and the average value was obtained to be 98.7 ps. This lifetime was attributed to the annihilation of positrons from the free state in diamond. For the synthesized type Ib specimen, the observed lifetime of positrons is longer than τ_f, but S is smaller than S_f. This fact was attributed to the annihilation of positrons trapped by the open spaces introduced by substitutional nitrogen atoms. For these specimens after electron irradiation, the species of the major vacancy-type defects was determined to be neutral and/or negatively charged monovacancies. The shallow trapping centres of positrons were also found to be introduced by the irradiation. For the natural type IIa and IIb specimens, the annihilation mode of positrons trapped by vacancy clusters was observed, and the size of open space of such defects was estimated to be $V_5 - V_7$. For the natural type IIb specimen, the observed temperature dependence of the trapping rate of the vacancy clusters was explained assuming that such defects act as compensators for acceptor impurities (boron).

References

[1] Field J E (ed) 1979 *The Properties of Diamond* (London: Academic)
[2] Freund A K 1995 *Opt. Eng.* **34** 432
[3] Fox B A, Hartsell M L, Malta D M, Wynands H A, Kao C-T, Plano L S, Tessmer G J, Henard R B, Holmes J S, Tessmer A J and Dreifus D L 1995 *Diamond Relat. Mater.* **4** 622
[4] Prawer S 1995 *Diamond Relat. Mater.* **4** 862
[5] Hautojärvi P and Vehanen A 1979 *Positrons in Solids* ed P Hautojärvi (Berlin: Springer) p 1
[6] Dannefaer S, Mascher P and Kerr D 1992 *Diamond Relat. Mater.* **1** 407
[7] Fujii S, Nishibayashi Y, Shikata S, Uedono A and Tanigawa S 1995 *Appl. Phys.* A **61** 331
[8] Uedono A, Kawano T, Tanigawa S, Suzuki R, Ohdaira T, Mikado T, Fujii S and Shikata S 1997 *Japan. J. Appl. Phys.* **34** 1772
[9] Nilen R W N, Lauff U, Connell S H, Stoll H, Siegle A, Schneider H, Castellaz P, Kraft J, Bharuth-Ram K, Sellschop J P F and Seeger A 1997 *Appl. Surf. Sci.* **116** 198
[10] Dannefaer S and Kerr D 1998 *Diamond Relat. Mater.* **7** 339
[11] Liu W, Berko S and Mills A P Jr 1992 *Mater. Sci. Forum* **105–110** 743
[12] Tanigawa S 1993 *Hyperfine Interact.* **79** 575
[13] Panda B K, Fung S and Beling C D 1996 *Phys. Rev.* B **53** 1251
[14] Amrane Na, Soudini S, Amrane N and Aourag H 1996 *Mater. Sci. Eng.* B **40** 119
[15] Schmidt W G and Verwoerd W S 1996 *Phys. Lett.* A **222** 275
[16] Nilen R W N, Connell S H, Britton D T, Fischer C G, Sendezera E J, Schaaff P, Schmidt W G, Sellschop J P F and Verwoerd W S 1997 *J. Phys.: Condens. Matter* **9** 6323
[17] Nishibayashi Y, Tomikawa T, Shikata S and Fujimori N 1994 *Trans. Mater. Res. Soc. Japan.* B **14** 1537
[18] West R N 1979 *Positrons in Solids* ed P Hautojärvi (Berlin: Springer) p 89
[19] Puska M J, Mäkinen S, Manninen M and Nieminen R M 1989 *Phys. Rev.* B **39** 7666
[20] Kirkegaard P, Eldrup M, Mogensen O E and Pedersen N J 1981 *Comput. Phys. Commun.* **23** 307
[21] Asoka-Kumar P, Lynn K G and Welch D O 1994 *J. Appl. Phys.* **76** 4935
[22] van Veen A, Schut H, de Vries J, Hakvoort R A and Ijpma M R 1990 *AIP Conf. Proc.* **218** 171
[23] Li Y S, Berko S and Mills A P Jr 1992 *Mater. Sci. Forum* **105–110** 739
[24] Uedono A, Kitano T, Hamada K, Moriya T, Kawano T, Tanigawa S, Suzuki R, Ohdaira T and Mikado T 1996 *Japan. J. Appl. Phys* **35** 2000
[25] Loubser J H N and van Wyk J A 1978 *Rep. Prog. Phys.* **41** 1201
[26] Isoya J 1989 *New Diamond* **5** 6
[27] Smith W V, Sorokin P P, Gelles I L and Lasher G J 1959 *Phys. Rev.* **115** 1546
[28] Krause-Rehberg R, Drost Th, Polity A, Roos G, Pensl G, Volm D, Meyer B K, Bischopink G and Benz K W 1993 *Phys. Rev.* B **48** 11 723
[29] Uedono A, Ujihira Y, Ikari A, Haga H and Yoda O 1993 *Hyperfine Interact.* **79** 615
[30] Uedono A, Wei L, Tanigawa S, Suzuki R, Ohgaki H, Mikado T, Kametani H, Akiyama H, Yamaguchi Y and Koumaru M 1993 *Japan. J. Appl. Phys.* **32** 3682
[31] Puska M J, Corbel C and Nieminen R M 1990 *Phys. Rev.* B **41** 9980
[32] Dyer H B and du Preez L 1965 *J. Chem. Phys.* **42** 1898
[33] Davies G and Hamer M F 1976 *Proc. R. Soc.* A **348** 285
[34] Davies G 1977 *Nature* **269** 498
[35] Isoya J, Kanda H, Uchida Y, Lawson S C, Yamasaki S, Itoh H and Morita Y 1992 *Phys. Rev.* B **45** 1436
[36] Dannefaer S 1990 *Defect Control in Semiconductors* ed K Sumino (North-Holland: Elsevier) p 1561
[37] Brauer G, Anwand W, Coleman P G, Störmer J, Plazaola F, Campillo J M, Pacaud Y and Skorupa W 1998 *J. Phys.: Condens. Matter* **10** 1147
[38] Uedono A, Ozaki K, Ebe H, Moriya T, Tanigawa S, Yamamoto K and Miyamoto Y 1997 *Japan. J. Appl. Phys.* **36** 6661
[39] Uedono A, Tanigawa S, Funamoto H, Nishikawa A and Takahashi K 1990 *Japan. J. Appl. Phys.* **29** 555
[40] Sharma S C, Dark C A, Hyer R C, Green M, Black T D, Chourasia A R, Chopra D R and Mishra K K 1990 *Appl. Phys. Lett.* **56** 1781
[41] Suzuki R, Kobayashi Y, Mikado T, Ohgaki H, Chiwaki M, Yamazaki T, Uedono A, Tanigawa S and Funamoto H 1992 *Japan. J. Appl. Phys.* **31** 2237
[42] Dannefaer S, Bretagnon T and Kerr D 1993 *Diamond Relat. Mater.* **2** 1479